# A reflection grating for atoms at normal incidence



1997 Europhys. Lett. 39 485

(http://iopscience.iop.org/0295-5075/39/5/485)

*Europhys. Lett.*, **39** (5), pp. 485-490 (1997)

# A reflection grating for atoms at normal incidence

A. Landragin, L. Cognet, G. Zs. K. Horvath
C. I. Westbrook, N. Westbrook and A. Aspect
*Institut d'Optique, URA 14 du CNRS - BP 147, F-91403 Orsay Cedex, France*

(received 7 May 1997; accepted in final form 22 July 1997)

PACS. 32.80Lg – Mechanical effects of light on atoms, molecules, and ions.
PACS. 32.80−t – Photon interactions with atoms.
PACS. 32.80Pj – Optical cooling of atoms; trapping.

**Abstract.** – We have observed efficient atomic diffraction at normal incidence on an evanescent standing wave with a very weak spatial modulation. A modulation as small as 1.5% causes 66% of the atoms to be diffracted into the orders $\pm 1$. The measured diffraction efficiencies agree quantitatively with a scalar treatment of diffraction in the thin phase grating approximation.

Ever since the pioneering experiments of ref. [1], atomic diffraction from laser standing waves has been an important element in atom optics. In particular, several groups have constructed atom interferometers using such gratings [2]. An interesting variant of this technique is to use a standing evanescent wave to create a reflection grating [3]. Recently, two groups have reported the observation of diffraction of an atomic beam at grazing incidence from such a grating [4]. Curiously, theoretical analyses that neglect the structure of the atomic ground state, *i.e.* representing the atoms as scalar de Broglie waves [5]-[7], predict a vanishingly small diffraction probability for these experiments. This is because at grazing incidence, the atom sees a rapidly alternating modulation during reflection which washes out the effect. On the other hand, these experiments can be explained by invoking a transfer between different ground state Zeeman sublevels, induced by an impurity of polarization, rather than by a purely scalar diffraction effect [8]. We have thus the paradoxical situation that a very intuitive and fundamental phenomenon, scalar diffraction from a reflection grating, has not yet been observed for de Broglie waves [9].

In this paper, we report on the observation of atomic diffraction at normal incidence on a spatially modulated evanescent wave with a pure TE or TM polarization. In this situation, a scalar wave description of the atoms [6] predicts efficient diffraction without transitions between different Zeeman sublevels. We have been able to compare quantitatively our experimental results with this scalar theory of diffraction. A remarkable result of this theory is that a very weak spatial modulation is enough to efficiently diffract the atoms.

In an evanescent-wave atomic mirror (fig. 1) the reflection is due to a potential barrier which is, in the large-detuning, low-saturation limit, equal to the atomic ground state light shift (*i.e.* to the square of the exponentially varying electric field). If the evanescent wave contains a standing wave component parallel to the plane of the mirror, the potential can be written as

$$U(x,z) = U_0\, e^{-2\kappa z}\left[1 + \varepsilon \cos\left(2k_x x\right)\right]\,, \tag{1}$$

where $\varepsilon$ is the contrast of the interference pattern, and $1/\kappa$ is the decay length of the electric field ($\kappa$ and $k_x$ are of order $k_L = 2\pi/\lambda_{\mathrm{L}}$, where $\lambda_{\mathrm{L}}$ is the vacuum wavelength of the laser which

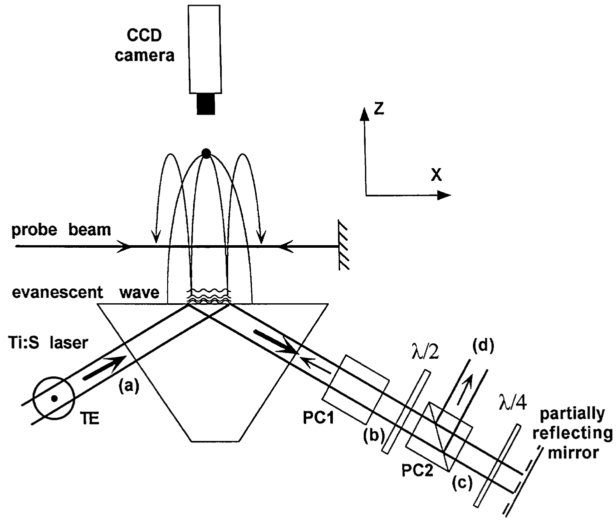


Fig. 1. – Schematic of the experiment. The titanium sapphire laser beam is TE polarized (perpendicular to the plane of the figure). The two polarizing beamsplitter cubes (PC) are identical; PC1 transmits the TE polarization. The partially reflecting mirror is a glass surface with a Fresnel coefficient of about 7%. The orientation of the two waveplates controls the amount of retroreflected light.

creates the evanescent wave). The corresponding equipotential surfaces are sinusoidal with a peak-to-peak height $\Delta z = \varepsilon/\kappa$. For the diffraction to be efficient, this height $\Delta z$ has to be on the order of the de Broglie wavelength, *i.e.* $\varepsilon \simeq \frac{\lambda_{\rm dB}}{\lambda_{\rm L}}$. Indeed, it has been shown that, to a good approximation, the grating behaves as a thin phase grating which produces a spatially modulated de Broglie wave whose corresponding phase modulation index is [6]

$$\varphi = \frac{2\pi\Delta z}{\lambda_{\rm dB}} = \varepsilon\frac{P_z}{\hbar\kappa}\,, \tag{2}$$

where $\lambda_{\rm dB}$ is the de Broglie wavelength associated with the normal (incident) atomic momentum $P_z$. The $n$-th diffraction order with a transverse momentum $2n\hbar k_x$ has an intensity $J_n^2(\varphi)$, where $J_n$ is the Bessel function of order $n$.

Our experimental setup is similar to that described in previous papers [10], [11]. We capture approximately $10^8$ atoms of $^{85}$Rb in a magneto-optical trap and release them 17.3 mm above the evanescent wave mirror. The evanescent wave results from total internal reflection of a laser beam (of intensity $I_{\rm L}$) in a prism of index of refraction $n_1 = 1.869$ (at 780 nm, *i.e.* the $D_2$ line of Rb used to reflect the atoms) at an incidence angle $\theta_1 = 53.4°$ $\left(k_x = k_{\rm L} n_1 \sin\theta_1 \simeq 1.5\; k_{\rm L} \text{ and } \kappa = k_{\rm L}\sqrt{n_1^2\;\sin^2\theta_1 - 1} \simeq 1.12\; k_{\rm L}\right)$. We retroreflect a small part, $I_{\rm R}$, of the laser beam which creates the evanescent wave. Both beams are TE polarized, with a purity better than $10^{-3}$ in intensity. The polarization of the evanescent wave is thus linear, so for a detuning large compared to the hyperfine structure of the $6P_{3/2}$ state, the light shifts of all the Zeeman sublevels of the $F = 3$ state are equal [11]. The modulated dipole potential is thus given by eq. (1) with $U_0 = \hbar\Lambda$, the light shift at the surface of the prism, and $\varepsilon$ the optical contrast given by $\varepsilon = 2\frac{\sqrt{R}}{1+R}$, with $R = I_{\rm R}/I_{\rm L}$. Since $\varepsilon$ depends only on $R$, it is constant over the whole surface of the mirror even with Gaussian beams, as long as the incident and retroreflected beams overlap precisely, both in size and position. We have adjusted the two sizes to be equal within 5% using their image on a CCD camera, and superimposed the two beams using the retroreflection through a spatial filter.

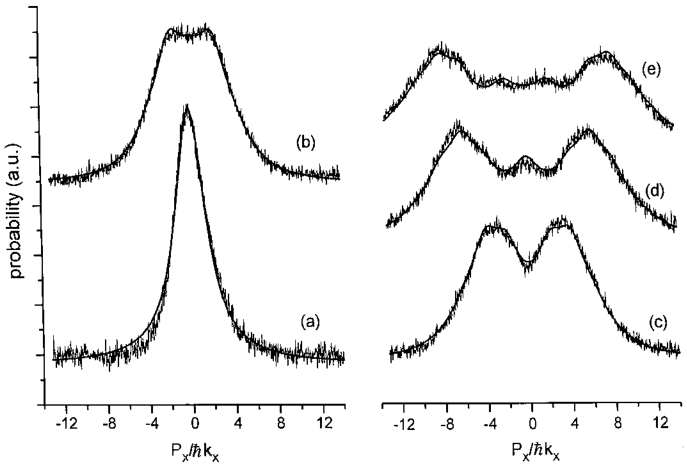


Fig. 2. – Atomic diffraction patterns for different values of the contrast of the TE evanescent standing wave: (a) zero contrast (beamstop in the retroreflected beam), (b) $\varepsilon = 0.0139$, (c) $\varepsilon = 0.0230$, (d) $\varepsilon = 0.0359$, (e) $\varepsilon = 0.0433$. The smooth solid lines represent the fits (Bessel functions convoluted by the resolution function of curve (a)).

Because the incident momentum of the atoms is large, $P_z = 87\ \hbar\kappa$ , we need to adjust $R$ to a small value, around $10^{-4}$, to be in the regime where $\varphi$ is on the order of 1. We do so by combining a weakly reflecting mirror, two polarizing cubes, and two waveplates (fig. 1). When the quarter waveplate is rotated through 45°, the total reflection coefficient $R$ varies between zero and a maximum value which is determined by the setting of the half waveplate. The maximum value $R_{\max} = 5 \times 10^{-4}$ ($\varepsilon_{\max} = 4.5 \times 10^{-2}$) is deduced from the measurement of the powers of the incident and retroreflected beams [12]. The intermediate values of $R$ are deduced from the measured orientation of the quarter waveplate, which is known with a 0.2° accuracy, leading to a maximum uncertainty of $4 \times 10^{-6}$ in $R$ ($3 \times 10^{-4}$ in $\varepsilon$).

To observe diffraction, we image the atoms onto a slow scan CCD camera (Princeton Instruments model ATE CCD 768 K) as they pass through a sheet of resonant light on their way back down after bouncing (fig. 1). Typical profiles, for different values of the contrast $\varepsilon$, are shown in fig. 2. The horizontal coordinate on the profiles has been converted to an equivalent momentum along the $x$-axis. The evolution of the profiles clearly suggests diffraction. Although our resolution is not sufficient to separate adjacent peaks, we can see, for example, the increase in the populations of the higher diffraction orders, while the population of the zeroth order first decreases (curves (b) and (c)), and then increases again (curve (d)), as expected for the $J_0^2$ function. These profiles were acquired after a fine adjustment of the superposition of the incident and retroreflected beams, otherwise the non-uniform contrast led to an asymmetry between the two peaks of the spatial distribution of the diffracted atoms [13].

The bottom curve (a) shows the atomic distribution with a beam stop in the retroreflected laser beam (zero contrast in the evanescent wave). Its width is determined by several factors. First, because of the size of the mirror (1 mm) and the short delay (100 ms) between the reflection and the detection, even a perfectly collimated atomic beam would show a width of 1 cm/s, *i.e.* a momentum spread of about $\hbar k_x$ (FWHM). Second, the finite trap size (0.8 mm) and mirror size result in an imperfect collimation of $2.7\hbar k_x$ FWHM. Finally, the reflection is not perfectly specular [10], contributing about $1.5\hbar k_x$ FWHM. The convolution of all these effects leads to the distribution observed in the absence of modulation (curve (a)). We fit this distribution to a Lorentzian, and use the fitted curve as a resolution function in our experiment. The corresponding resolution in momentum space is $3.4\hbar k_x$ FWHM [14].

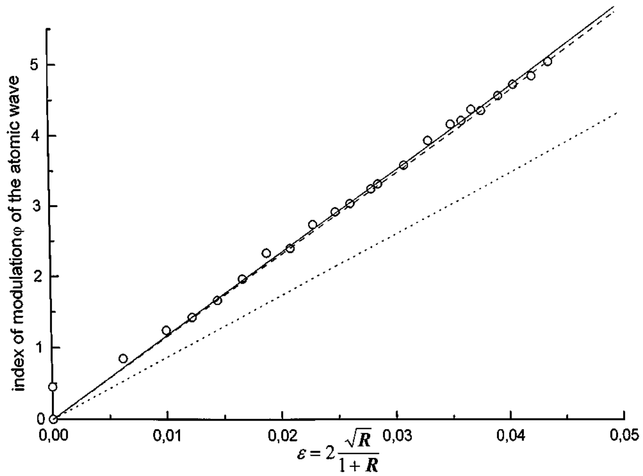


Fig. 3. – Phase modulation index $\varphi$ of the reflected atomic de Broglie waves deduced from the diffraction profiles as a function of the contrast $\varepsilon$ of the spatially modulated evanescent wave (TE polarization). The circles represent the modulation indices deduced from the fits of the diffraction patterns, for values of $\varepsilon$ calculated from the measured reflection coefficient $R$ of the laser beam. The solid line shows the fit to the data points. The dashed (dotted) line shows the theoretical prediction with (without) the van der Waals force taken into account. The second point for $\varepsilon = 0$ (with $\varphi \neq 0$) is obtained for a rotation of the $\lambda/4$ plate corresponding to a minimum retroreflected intensity (this is different from curve (a) of fig. 2). The index of modulation deduced from the fit is consistent with a stray retroreflection of $3 \times 10^{-6}$, probably from reflections on the interfaces of the cubes and waveplates.

To calculate the expected diffraction patterns, we first consider an incident atomic plane wave [6]: in the case of normal incidence, the spectrum consists of diffraction peaks of momentum $P_{x,n} = 2n\hbar k_x$ with a population $J_n^2(\varphi)$. We convolute these delta functions with our Lorentzian resolution function and sum over the orders $n = -6$ to $+6$. This calculated pattern can be fitted to our experimental profiles with the modulation index $\varphi$, and a vertical scaling factor as the only adjustable parameters (see solid lines in fig. 2). We have plotted (circles in fig. 3) the fitted value of the phase modulation index $\varphi$ as a function of the optical contrast $\varepsilon$ deduced from the measurement of $R$. The individual uncertainties of the data points in fig. 3 are only due to the precision in the $\lambda/4$ rotation and in the fit (<3%). The observed linear variation of $\varphi$ with $\varepsilon$ is an important test of our model in which the diffraction is due to the modulation of the evanescent wave resulting from the interference between incident and retroreflected evanescent waves.

We have fitted the data points to a straight line (solid line in fig. 3) and have found a slope of 117. This slope is 1.35 times steeper than the expected slope, $\frac{P_z}{\hbar\kappa} = 87$ (dotted line in fig. 3). The discrepancy is inconsistent with our uncertainty in the expected slope, which includes: 5% for the measurements of the maximum contrast (see [12]) and the relative sizes of the two beams, 1% for the incident momentum, and 2% in the value of $\kappa$ (due to the uncertainty in the angle of incidence $\theta_1$).

To understand this difference we must take into account the van der Waals potential between the atoms and the dielectric surface supporting the evanescent wave [11], which increases the diffraction efficiency for the same $R$. This can be understood qualitatively because the van der Waals potential causes the slope of the total potential $\mathrm{d}U/\mathrm{d}z$ to decrease, and the atoms to spend more time in the evanescent wave. In the calculation of the diffraction efficiency, this effect leads to an increase in the index of modulation by a factor, which depends on the dipole potential, thus leading to a dependence on the absolute value of the light shift $\Lambda$ and not only on $\varepsilon$ (*i.e.* on $R$). This effect diminishes for larger dipole potentials, but since we use Gaussian laser beams, there is always a large fraction of the atoms that bounces on the edge of the mirror where the van der Waals force has a strong influence.

In fact, we have found numerically that in our range of experimental parameters the effect of the van der Waals interaction is chiefly sensitive to the ratio between the maximum of the total reflecting potential (light shift plus van der Waals) at the center of the Gaussian profile, and the reflection threshold (the minimum potential barrier necessary to reflect the atoms). We therefore do not need the absolute value of the light shift, which is more difficult to measure precisely [15]. In the experiment, we first determine the intensity corresponding to the reflection threshold, and then we increase it by 10%. This information allows us to calculate a corrected value of the modulation index at each point on the mirror. To get the diffraction pattern, we perform an average over the mirror. This results in a functional form for the diffraction pattern that is more complex than a simple sum of Bessel functions. However, within our experimental resolution, we cannot distinguish the corrected diffraction pattern from a simple sum of Bessel functions with a new effective modulation index, equal to 1.33 times the previous one (the correction factor is constant over all our range of parameters). The resulting expected slope is 115 (dashed line in fig. 3), which is in good agreement with the experimental slope, 117. The uncertainty in the calculated slope must now take into account the uncertainty in the threshold of the reflection (5%), which leads a total uncertainty of $\binom{+7\%}{-10\%}$.

We have also performed the experiment with TM polarization in both incident and retroreflected laser beams. The observed spatial distributions of the diffracted atoms are qualitatively similar to the TE case, but for values of $R$ larger by a factor of about 40. To understand this difference, we note that the polarizations in the counterpropagating evanescent waves are elliptical in the plane of incidence ($xz$), with opposite senses of rotation, and the resulting polarization has an ellipticity modulated both in magnitude and orientation. In the limit of a detuning large compared to the excited state hyperfine structure, and for our case of a ground state hyperfine level with $J = 1/2$ , the $m_\mathrm{F}$ Zeeman sublevels (relative to the $y$-axis, perpendicular to the plane of the elliptic polarization) remain eigenstates of the light shift operator. This results in a different light shift modulation for each Zeeman sublevel.

Our quantitative calculations of the profiles also account for the fact that the effective mirror size is different for each Zeeman sublevel, as well as the effect of the van der Waals interaction. The profiles calculated for each Zeeman sublevel are then averaged assuming a uniform distribution among the sublevels. Unlike the TE case, the profiles calculated in this way differ from a simple sum of Bessel functions, and fit the experimental profiles more closely. After taking all these effects into account, the observed diffraction patterns are in good agreement with theory.

We have thus found that atomic diffraction at normal incidence on a spatially modulated evanescent wave with a pure TE or TM polarization can be quantitatively understood using the scalar diffraction theory developed in ref. [6]. We now plan to investigate the effect of different polarizations for the incident and reflected evanescent waves, as well as the influence of the angle of incidence. This should help clarify the phenomenon of diffraction at grazing incidence.

We have also shown that efficient atomic diffraction can be observed even for very weak retroreflected beams: 66% of the atoms are in the $\pm 1$ orders for $R = 5.6 \times 10^{-5}$. The great sensitivity of atomic mirrors to stray light is illustrated by the fact that a reflection coefficient $R$ as small as a few $10^{-6}$ results in a noticeable effect. One must be aware of this great sensitivity when performing atom optics experiments using evanescent wave atomic mirrors at normal incidence.

***

We are grateful to N. Dimarcq of Laboratoire de l'Horloge Atomique (Orsay) for the loan of the slow scan CCD camera. GZsKH is supported by the Swiss National Science Foundation. This work was supported by DRET, Région Ile de France, Ultimatech (CNRS), and the HCM and TMR programs of the European Union.

REFERENCES

[1] Gould P. L., Ruff G. A. and Pritchard D. E., *Phys. Rev. Lett.*, **56** (1986) 827; see also Gould P. L. and Pritchard D. E., *Proceedings of the International School of Physics "Enrico Fermi", course CXXXI*, edited by A. Aspect, W. Barletta and R. Bonifacio (IOS Press, Amsterdam) 1996 and references therein.

[2] Rasel E. M., Oberthaler M. K., Batelaan H., Schmiedmayer J. and Zeilinger A., *Phys. Rev. Lett.*, **75** (1995) 2633; Giltner D. M., McGowan R. W. and Lee S. A., *Phys. Rev. Lett.*, **75** (1995) 2638.

[3] Hajnal J. V. and Opat G. I., *Opt. Commun.*, **71** (1989) 119; Feron S., Reinhardt J., Ducloy M., Gorceix O., Chormaic S. N., Miniatura C., Robert J., Baudon J., Lorent V. and Haberland H., *Phys. Rev. A*, **49** (1994) 4733; Stenlake B. W., Littler I. C. M., Bachor H.-A., Baldwin K. G. H. and Fisk P. T. H., *Phys. Rev. A*, **49** (1994) 16.

[4] Christ M., Scholz A., Schiffer M., Deutschmann R. and Ertmer W., *Opt. Commun.*, **107** (1994) 211; Brouri R., Asimov R., Gorlicki M., Feron S., Reinhardt J., Lorent V. and Haberland H., *Opt. Commun.*, **124** (1996) 448.

[5] Deutchmann R., Ertmer W. and Wallis H., *Phys. Rev. A*, **47** (1993) 2169.

[6] Henkel C., Courtois J.-Y. and Aspect A., *J. Phys. II*, **4** (1994) 1955.

[7] Savage C. M., Gordon D. and Ralph T. C., *Phys. Rev. A*, **52** (1995) 4741.

[8] Gordon D. and Savage C. M., *Opt. Commun.*, **130** (1996) 34; Gordon D. and Savage C. M., *Opt. Commun.*, **136** (1997) 503. See also Henkel C., Mølmer K., Kaiser R. and Westbrook C. I., *Phys. Rev. A*, **56** (1997) 1; Deutchmann R., Ertmer W. and Wallis H., private communication.

[9] In the time domain, diffraction at normal incidence, interpretable by a scalar theory, has been observed, and used for atomic interferometry (see Steane A., Szriftgiser P., Desbiolles P. and Dalibard J., *Phys. Rev. Lett.*, **74** (1995) 4972; Szriftgiser P., Guéry-Odelin D., Arndt M. and Dalibard J., *Phys. Rev. Lett.*, **77** (1996) 4).

[10] Landragin A., Labeyrie G., Henkel C., Kaiser R., Vansteenkiste N., Westbrook C. I. and Aspect A., *Opt. Lett.*, **21** (1996) 1591.

[11] For a discussion of the role of the van der Waals interaction in the evanescent wave mirror see Landragin A., Courtois J.-Y., Labeyrie G., Vansteenkiste N., Westbrook C. I. and Aspect A., *Phys. Rev. Lett.*, **77** (1996) 1464 and references therein.

[12] The maximum reflection coefficient is determined by the ratio $R_{\max} = P_d\,P_c/P_a\,P_b$, where $P_a$, $P_b$, $P_c$ are the measured powers of the incident beam at points (a), (b) and (c) of fig. 1, and $P_d$ is the maximum power measured at point (d), as a function of the orientation of the quarterwave plate. $P_d$ is also equal to the maximum power of the retroreflected beam at point (b).

[13] To understand how a non-uniform index of modulation can lead to an asymmetry in the atomic spatial distribution, one has to take into account the correlation between the position where the atoms bounce on the mirror, their incident momentum and the position where they are detected in the probe beam.

[14] The fact that our collimation is of the same order as the expected momentum transfer corresponds to a transverse coherence length which is approximately equal to that of the grating period. In other words, our diffraction pattern does not result from multiple-beam interference.

[15] The value of the total potential maximum deduced from the threshold measurement is 14% higher than the value deduced from the direct evaluation of the light shift, based on: power of the incident laser beam 2.1 W, size of the beam waists $0.88 \times 0.82$ mm, detuning 3 GHz, angle $\theta_1 = 53.4^\circ$. This is consistent with our 20% uncertainty in this light shift measurement.